Acoustic emission in bulk normal and superfluid ^{3}He

M. T. Noble,[1, a)] Š. Midlik,[2] L. Colman,[1] D. Schmoranzer,[2] and V. Tsepelin[1]
[1)] *Department of Physics, Lancaster University, Lancaster, LA1 4YB, UK*
[2)] *Faculty of Mathematics and Physics, Charles University, Prague, Czech Republic*

We present measurements of the damping experienced by custom-made quartz tuning forks submerged in ^{3}He covering frequencies from 20 kHz to 600 kHz. Measurements were conducted in the bulk of normal liquid ^{3}He at temperatures from 1.5 K down to 12 mK and in superfluid ^{3}He-B well below the critical temperature. The presented results complement earlier work on tuning fork damping in ^{3}He, removing possible ambiguities associated with acoustic emission within partially enclosed volumes and extend the probed range of frequencies, leading to a clearly established frequency dependence of the acoustic losses. Our results validate existing models of damping and point toward the same mechanism of wave emission of first sound in normal ^{3}He and liquid ^{4}He and zero sound in superfluid ^{3}He. We observe a steep frequency dependence of the damping $\approx f^{5.5}$, which starts to dominate around 100 kHz and restricts the use of tuning forks as efficient sensors in quantum fluids. The acoustic emission model can predict the limiting frequencies for various devices, including MEMS/NEMS structures developed for quantum turbulence and single vortex dynamics research.

The general form of motion of quantum fluids such as superfluid phases of helium isotopes ^{4}He and ^{3}He, quantum turbulence, has sparked scientific interest since its discovery in the middle of the last century. Close analogies to turbulence in classical fluids have been formulated, focusing on large flow structures, while fundamental differences exist that highlight the unique nature of such flow[1]. A significant part of experimental research of quantum turbulence focuses today on the use of submerged electro-mechanical resonators of micron and submicron dimensions. The goal here is to manufacture devices with the ability to interact with a single quantized vortex[2], providing experimental access to probing its dynamics which hold the key to some of the most important outstanding questions, such as how vortices interact with solid structures and how kinetic energy is dissipated in a fluid with zero viscosity. Single vortex sensing can be achieved by lowering the dimensions and mass of a mechanical resonator (beam, wire, tuning fork, ...) and probing the energy dissipation at the lowest attainable length scales[3–5]. Recently, this development has been made possible by the improved accessibility of nanofabrication facilities allowing for custom production of devices of various shapes and dimensions[2,6–11] based on materials such as monocrystalline silicon, silicon nitride, quartz glass or thin layers of superconducting metals.

When designing such a detector, it is crucial to understand the behaviour of the device itself and its interaction with the fluid in the relevant dynamical regimes, especially with numerous dissipative mechanisms affecting its sensitivity. First, it is necessary to evaluate the intrinsic damping of the device, as measured in a low temperature vacuum. Defects in the crystal lattice, such as two-level systems[12] present at grain boundaries or interfaces can contribute to this damping, as well as any clamping losses due to finite acoustic transmission through the supports. Submerged devices additionally experience a generally temperature dependent "background" damping in the hydrodynamic[13] and ballistic regimes[14,15] of the working fluid. Finally, any submerged oscillating body emits sound waves in the fluid, and acoustic damping[16,17] becomes especially important at high frequencies, imposing a severe practical limit on the design and usability of such devices.

All the mentioned regimes were recently explored systematically using quartz tuning forks[18] in ^{4}He and to a lesser extent[19] in ^{3}He. The results for ^{4}He provide a robust validation of the models for both normal liquid and superfluid phases. Here we provide bulk measurements of acoustic damping of quartz tuning forks in ^{3}He, covering the frequency range from 20 kHz to 600 kHz, and remove any ambiguities associated with acoustic emission inside a partially enclosed volume present in the earlier study[19]. Furthermore, the data shown validates the applicability of a single acoustic emission model for both ^{4}He and ^{3}He liquids, including the superfluid phases He-II and ^{3}He-B. Considering the differences in the behaviour of the two helium isotopes due to their bosonic (^{4}He) versus fermionic (^{3}He) nature, this finding points towards similar mechanisms of acoustic wave emission in the mentioned classical and quantum fluids.

The measurements were conducted using a custom-made[20] array of quartz tuning forks[18,19,21,22] consisting of five devices connected in parallel, sharing electrical leads. The fundamental and the first overtone resonant frequencies of each fork were determined by varying the fork length from 1.9 mm to 0.9 mm in order to cover a wide range of frequencies while ensuring sufficient frequency spacing between the resonances to avoid any cross-talk. All of the remaining dimensions, see Figure 1, were common for all of the forks namely, prong width $T = 90\,\mu$m, thickness $W = 75\,\mu$m given by wafer thickness, and prong spacing $D = 90\,\mu$m.

For mechanical rigidity and easy manipulation, the fork array was glued between two Stycast 1266 impregnated papers, and an electrical connection was realized via soldering device contacts to copper leads representing also the only thermal link in the case of measurements

[a)] Electronic mail: t.noble@lancaster.ac.uk

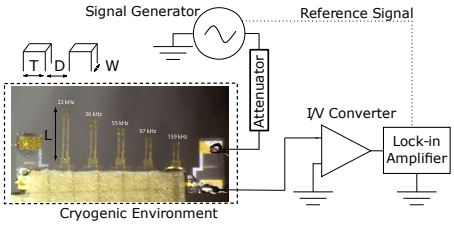

FIG. 1. Photograph of the tuning fork array and a schematic connection diagram.

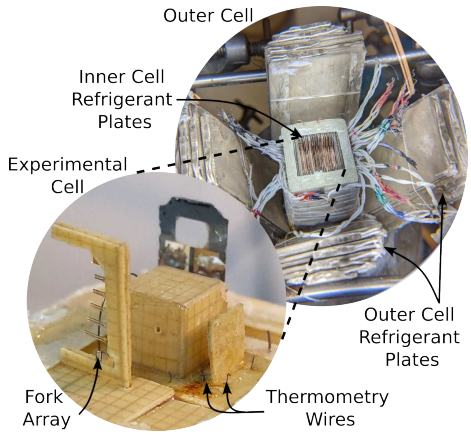

FIG. 2. Photograph of the open double-wall demagnetization cell. The inner cell contains the tuning fork array and thermometry. Copper plates, the refrigerant of the demagnetization stage, covered with silver sinter present in the inner and outer cells are visible.

under vacuum. All vacuum measurements characterizing the device intrinsic damping were performed using a dipstick submerged directly into a ^{4}He transport Dewar at 4.2 K. The intrinsic damping varied within an order of magnitude depending on the position of the fork in the array, pointing towards the importance of the base rigidity. For liquid ^{3}He measurements, the fork array was enclosed inside a Stycast cell[23] shown in Figure 2, containing also 80 silver-sintered copper plates of the nuclear demagnetization stage, mounted on the Lancaster advanced dilution refrigerator[24], allowing us to reach temperatures down to 100 µK. The cell was kept at nearly zero pressure and included vibrating wires used for thermometry[25].

The basic principle of the measurements relies on the piezo-electric properties of quartz[26] and the connection scheme is illustrated in Figure 1. Oscillatory movement of the fork prongs, in anti-phase with respect to each other, is induced by the driving voltage, using an Agilent 33521A function generator with output attenuated by 60 dB. The device response results in an ac current proportional to the velocity amplitude of the prong tip. The resulting current signal is first amplified and converted to a voltage using a custom I-V converter[27] with gain 10^6 and then detected by phase-sensitive lock-in amplifiers SR830 or SR844, depending on the measured frequency.

In order to describe the behaviour of an oscillating structure submerged in a liquid, it is necessary to introduce theoretical models of its damping for all relevant flow regimes. First, it is needed to characterize the intrinsic damping, measured in vacuum at low temperatures, caused solely by the mechanical structure of the oscillator. Additional temperature and frequency-independent contributions to the damping may be considered, such as magnetic losses and eddy current heating if using a magneto-motive driving scheme[28].

In the presence of a working fluid, additional dissipation of hydrodynamic origin appears. The intrinsic damping Δf_0 being well below or at most comparable to the hydrodynamic damping Δf_H is typically considered a necessary condition for the device to be used as a detector. The temperature- or frequency-dependent hydrodynamic contributions to the total damping originate from multiple effects and must be considered separately. In this work, we describe only the laminar/potential flow regime of the normal/superfluid components at velocities below any turbulent instability. It is known that losses due to acoustic emission dominate at high frequencies[16,17]. Damping of the submerged oscillator at frequencies well below this point is well understood and described either by viscous drag in the normal liquid phase or the two-fluid regime of the superfluid phase or at even lower temperatures (for ^{3}He below $\simeq 0.25T_C$) by the frequency-independent ballistic drag.

Although modelling the ballistic drag in superfluid ^{3}He is generally a nontrivial task due to the effects of Andreev reflection[29] reducing the resulting damping force on a moving object, it may be derived for the case of simplified geometries and low velocities[19]. In the viscous drag regime, both the width (corresponds to the damping) and resonant frequency (linked to the mass) of the oscillator's resonance are affected by the fluid. The decrease of the resonant frequency f_H with respect to its vacuum value f_0 is caused by the fluid back-flow and by the mass enhancement due to the creation of a Stokes boundary layer[13]. For boundary layer thicknesses well below the oscillator dimensions[22], the solution for an incompressible liquid leads to the square-root frequency dependence of the viscous contribution to the resonance width[30]:

$$\Delta f_\mathrm{H} = C\frac{S}{2m_\mathrm{eff}}\sqrt{\frac{\rho_\mathrm{nf}\eta f_0}{\pi}}\left(\frac{f_\mathrm{H}}{f_0}\right)^2, \qquad (1)$$

where C denotes a geometrical factor of the order of unity, S is the prong surface area, m_eff the effective mass of the oscillator, and ρ_nf and η are temperature dependent density of the normal fluid component and helium

viscosity, respectively. The model describes the system accurately when considering the high-frequency limit i.e. when oscillator characteristic dimensions greatly exceed the viscous penetration depth δ_n given by $\sqrt{\eta/\rho_{\rm nf} f_0 \pi}$. Further corrections accounting for large δ_n are needed when approaching the superfluid transition in ^{3}He due to a steep rise of helium viscosity[14,30] and slip effects need to be considered in transitional flow between the hydrodynamic and ballistic regimes.

At high frequencies, however, the above-mentioned damping will be negligible compared to energy losses due to the emission of acoustic waves. In order to describe the behaviour of the resonator correctly, a suitable model of acoustic emission must be considered[16]. For acoustic emission by a tuning fork in liquid ^{4}He a "3D" model presented in[16] is the most successful in describing the experimental data. The tuning fork is modelled as a linear quadrupole of planar sources with effective strength based on the mode-dependent velocity distribution. In the model, emission of spherical waves is considered, leading to the following solution in form of spherical Bessel functions j_m:

$$\Delta f^{3D} = C_{3D} \frac{\rho_{\rm H}}{c} \frac{W^2 L_{\rm eff}^2}{m_{\rm eff}} \frac{f_{\rm H}^4}{f_0^2} \times \sum_{\substack{m=0,\\ \text{even}}}^{\infty} (2m+1) \left[j_m\left(\frac{\pi f_{\rm H}(2T+D)}{c}\right) - j_m\left(\frac{\pi f_{\rm H} D}{c}\right)\right]^2 \quad (2)$$

with total helium density $\rho_{\rm H}$, sound velocity c, a geometrical factor of the order of unity C_{3D} and effective prong length $L_{\rm eff}$. In the long wavelength limit, using Taylor expansion, equation 2 yields the steep $\approx f^6$ dependence of the acoustic drag, which starts to dominate around 100 kHz for typical tuning forks[18] in ^{4}He.

To correctly account for the velocity distribution along the prong, it is necessary to introduce the mode-dependent prefactors $\xi_{\rm eff}$, $\mu_{\rm eff}$ giving the effective mass $m_{\rm eff} = \xi_{\rm eff} m$ and effective length $L_{\rm eff} = \mu_{\rm eff} L$. Their values for a cantilever may be derived based on[16,18] giving $\mu_{\rm eff} = 0.3915$ for the fundamental resonance and $\mu_{\rm eff} = 0.2169$ for the first overtone, while $\xi_{\rm eff} = 1/4$ for both modes.

In order to describe the sound emission in liquid ^{3}He, the previous work of the Lancaster group[19] gives a strong hint towards the applicability of the introduced model for both quantum liquids. Albeit, the results clearly show an effect of the resonator confinement resulting in the suppression of the sound emission for the part of the frequency range coinciding with the cavity dimensions.

Finally, when discussing acoustic emission in quantum fluids, it is necessary to distinguish between different sound modes. In bulk liquid ^{4}He it is first sound, a pressure wave, and second sound[31], a temperature wave, that must be considered. Due to the driving mechanism being a moving rigid wall, first sound emission is stronger than second sound emission by several orders of magnitude in the described experiments and second sound is not discussed further. Considering the fermionic nature of ^{3}He, sound waves may be regarded as deformations of the Fermi sphere, with first sound corresponding to a symmetric "breathing" mode and the so-called Landau zero sound mode[32] being described as asymmetric deformations. Second sound mode is strongly suppressed due to the very high viscosity of the normal component. The preference for first sound or zero sound depends on the frequency of oscillation ω and on the temperature, which affects the fluid relaxation time τ. The emission of zero sound is relevant only in the collisionless limit[33] $\omega\tau \gg 1$, and values of $\omega\tau$ for the forks at $0.16T_c$ are given in Table I. In normal ^{3}He $\omega\tau$ remains below 0.04 even for the highest frequency at all investigated temperatures. Two types of zero sound are known to propagate in superfluid ^{3}He-B, a longitudinal mode and a transverse mode. The transverse mode is not expected to propagate at low pressures[33]. The speed of the longitudinal mode here is 190 m s^{-1}, increased from that of first sound by 6 m s^{-1}.

TABLE I. Vacuum properties of fundamental and overtone resonant modes of used tuning forks measured at 4.2 K. The last column shows the product of the angular frequency, ω and the estimated relaxation time τ in superfluid ^{3}He-B at $0.16\,T_C$. This relaxation time represents the thermalization of individual quasiparticles to the walls of the cell and is obtained by dividing the mean free path of order 1 cm by the root mean square group velocity determined from $< v_g^2 > \simeq 2 v_{\rm F}^2 k_B T/\Delta$, where $v_{\rm F}$ is the Fermi velocity and Δ is the energy gap.

Fork-mode	Frequency Hz	Width Hz	$\omega\tau$ (T=0.16T_C)
L1-fund	22 403	0.05	56.1
L2-fund	35 770	5.15	89.7
L3-fund	55 276	0.29	139
L4-fund	97 055	3.58	243
L5-fund	159 316	0.55	399
L1-over	138 689	0.44	348
L2-over	220 110	32	552
L3-over	337 514	3.90	846
L4-over	579 000	159	1450

All measurements presented in this work were conducted in bulk liquid ^{3}He. Prior to the experiments on the demagnetization refrigerator, we characterized the intrinsic damping of each fork in vacuum at ≈4.2 K. The vacuum widths of individual forks differed by up to one order of magnitude, see Table I, which was caused most likely by the differences in the rigidity of the base at each tuning fork site. The obtained vacuum widths, with values comparable to the measurements in ballistic regime on superfluid ^{3}He at the lowest temperature, were subtracted from all data sets presented below. The differences in intrinsic damping between 4.2 K and low temperatures are negligible in comparison with the dominant acoustic or viscous losses.

In Figure 3 we summarize the experimentally obtained

resonant widths using the fork's fundamental and first overtone modes. Each point in the graph results from the resonant peak fit for the resonant frequency and full width at half height. Presented data were obtained from the measurements at five temperatures in normal liquid ^{3}He ranging from 1.5 K down to 12.4 mK and 0.16 T_C in the ballistic regime of superfluid ^{3}He.

For measurements in normal ^{3}He, we have evaluated the viscous hydrodynamic drag contribution by fitting the data to equation 1, shown in Figure 3 as dashed lines. The fits exclude points at frequencies above 100 kHz, where the acoustic damping becomes significant. Using experimental values of resonant frequency shift in liquid f_H/f_0, known values[30,34] of ρ_{nf} and η for ^{3}He and dimensions of the used tuning forks, we can evaluate a corresponding geometric C coefficient for each tuning fork for both resonant modes separately and at each temperature. The obtained values of C coefficients vary by less than 1% for different forks considering both their modes and by less than 3% across all the measured temperatures. The resulting temperature and frequency independent value $C = 0.65$ is in reasonable agreement with previous experiments[19] using tuning forks in partially enclosed volumes of normal liquid ^{3}He. The constant C is determined by the fork geometry and may be affected by the ratio of the viscous penetration depth to the tine dimensions, usually falling between 0.5 and 0.65, with higher values possible for short, high-frequency forks[18,22].

Subtracting the viscous drag contribution, we have performed the fits of the acoustic contribution based on Eq. (2), for all measured temperatures in normal and superfluid ^{3}He states. We have used known ^{3}He properties with first sound and zero sound velocities taken from[33,35], and measured properties of the tuning forks, leaving the geometric prefactor C_{3D} as the only fitting parameter. As the two resonant modes used have different velocity distributions along the prong length, we consider fundamental and overtone data sets separately. For normal liquid ^{3}He practically all experimental points usable for the acoustic contribution evaluation come from the overtone mode. Only for the superfluid ^{3}He data, can we distinguish the two modes using the derived values of μ_{eff}.

The model describes the observed damping with good accuracy, with values of geometrical coefficients for overtone and fundamental resonant modes $C_{3D}^{\text{ovt}} = 8.5$, with deviation of 20% between the measured temperatures and $C_{3D}^{\text{fund}} = 3.3$. In Figure 3 we show resulting curves (dotted lines) describing the total measured widths as a sum of viscous/ballistic and acoustic contributions based on the performed fits. The value obtained for the fundamental mode agrees quite well with results from superfluid ^{4}He[18], where $C_{3D} = 2.17$ was obtained. We note that the analysis in Ref.[18] uses the same effective prong length $\mu_{\text{eff}} = 0.3915$ for both the fundamental resonance and the first overtone, while the data dominated by acoustic damping come mostly from overtone measurements. After adjustment for the correct effective prong length $\mu_{\text{eff}} = 0.2169$, a prefactor of $C_{3D} = 7.1$ is obtained in ^{4}He, in good agreement with the present value $C_{3D}^{\text{ovt}} = 8.5$.

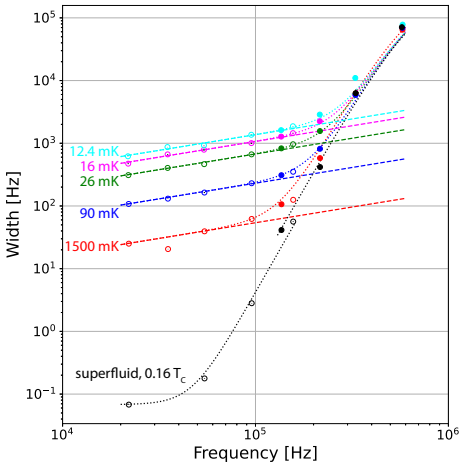

FIG. 3. Measured damping width minus the intrinsic contribution Δf_0 as a function of tuning fork frequency at five temperatures in normal liquid ^{3}He and one temperature in superfluid ^{3}He-B. Empty and filled circles represent fundamental and overtone resonant modes, respectively. Dashed lines correspond to the viscous drag contribution using fitted value of the geometrical parameter $C = 0.65$. The dotted lines represent fits of total resonance width as a sum of viscous drag and acoustic emission contributions. For the superfluid ^{3}He data we obtained different geometrical coefficients describing acoustic emission by fundamental resonant mode $C_{3D}^{\text{fund}} = 3.3$ and overtone resonant mode $C_{3D}^{\text{ovt}} = 8.5$.

The results confirm the validity of the model of acoustic emission by quartz tuning forks presented in[16] for the bulk normal liquid ^{3}He and superfluid ^{3}He-B in addition to the previous results in liquid ^{4}He. The values of geometrical coefficients, representing the only fitting parameters in the viscous drag and acoustic emission models are in good agreement with previous results. It is important to point out that the single value of the geometrical coefficient can describe acoustic emission in the whole range of temperatures in both quantum liquids. Our results, therefore, point toward the same mechanism of wave emission of the first sound in normal ^{3}He and liquid ^{4}He and longitudinal zero sound in superfluid ^{3}He-B, expected to dominate at the temperature and frequencies used. In addition, we showed that resonant modes with different velocity profile along the tuning fork prong must be considered separately. Complementing previous

experiments, this work brings together proof of the general validity of acoustic emission models, derivable for resonators of various shapes and sizes. Predictions of ballistic, viscous and acoustic damping obtained from the models can be expected to hold across a wide frequency range in all classical fluids and in quantum fluids as long as the coherence length is lower than the size of the oscillator.

ACKNOWLEDGMENTS

The research leading to these results has received funding from: the Czech Science Foundation under Project GAČR 20-13001Y; the European Union's Horizon 2020 Research and Innovation Programme, under Grant Agreement No. 824109, the European Microkelvin Platform (EMP); and the United Kingdom Science and Technology Funding Council grant number ST/T006773/1.

AUTHOR DECLARATIONS

Conflict of Interest

The authors have no conflicts to disclose.

Author Contributions

M. T. Noble: Conceptualization (equal); Data Curation (lead); Investigation (equal); Project Administration (lead); Writing - Review & Editing (equal). **Š. Midlik:** Conceptualization (equal); Data Curation (supporting), Formal Analysis (lead); Investigation (equal); Methodology (equal); Writing - Original Draft (equal); Writing - Review & Editing (equal). **L. Colman:** Conceptualization (equal); Data Curation (supporting); Formal Analysis (equal); Investigation (equal). **D. Schmoranzer:** Conceptualization (equal); Formal Analysis (equal); Funding Acquisition (lead); Methodology (equal); Project Administration (equal); Supervision (equal); Writing - Original Draft (equal); Writing - Review & Editing (equal). **V. Tsepelin:** Conceptualization (equal); Investigation (equal); Project Administration (equal); Supervision (equal); Writing - Review & Editing (equal).

DATA AVAILABILITY

The data that support the findings of this study are openly available at the Lancaster University Data Repository at https://doi.org/, reference number [XX].

[1] L. Skrbek, D. Schmoranzer, Š. Midlik, and K. R. Sreenivasan, "Phenomenology of quantum turbulence in superfluid helium," Proc. Natl. Acad. Sci. U.S.A **118**, e2018406118 (2021).
[2] A. Guthrie, S. Kafanov, M. T. Noble, Yu. A. Pashkin, G. R. Pickett, V. Tsepelin, A. A. Dorofeev, V. A. Krupenin, and D. E. Presnov, "Nanoscale real-time detection of quantum vortices at millikelvin temperatures," Nat. Commun. **12**, 2645 (2021).
[3] M. Leadbeater, D. C. Samuels, C. F. Barenghi, and C. S. Adams, "Decay of superfluid turbulence via Kelvin-wave radiation," Phys. Rev. A **67**, 015601 (2003).
[4] T. P. Simula, T. Mizushima, and K. Machida, "Kelvin waves of quantized vortex lines in trapped Bose-Einstein condensates," Phys. Rev. Lett. **101**, 020402 (2008).
[5] E. B. Sonin, "Symmetry of Kelvin-wave dynamics and the Kelvin-wave cascade in the $T = 0$ superfluid turbulence," Phys. Rev. B **85**, 104516 (2012).
[6] A. Kraus, A. Erbe, and R. H. Blick, "Nanomechanical vibrating wire resonator for phonon spectroscopy in liquid helium," Nanotechnology **11**, 165 (2000).
[7] M. Defoort, K. J. Lulla, T. Crozes, O. Maillet, O. Bourgeois, and E. Collin, "Slippage and boundary layer probed in an almost ideal gas by a nanomechanical oscillator," Phys. Rev. Lett. **113**, 136101 (2014).
[8] T. Kamppinen and V. B. Eltsov, "Nanomechanical resonators for cryogenic research," J. Low Temp. Phys. **196**, 283–292 (2019).
[9] I. Golokolenov, B. Alperin, B. Fernandez, A. Fefferman, and E. Collin, "Fully suspended nano-beams for quantum fluids," J. Low Temp. Phys. (2022), 10.1007/s10909-022-02722-y.
[10] E. Collin, L. Filleau, T. Fournier, Y. M. Bunkov, and H. Godfrin, "Silicon vibrating wires at low temperatures," J. Low Temp. Phys. **150**, 739–790 (2008).
[11] Š. Midlik, J. Sadílek, Z. Xie, Y. Huang, and D. Schmoranzer, "Silicon Vibrating Micro-Wire Resonators for Study of Quantum Turbulence in Superfluid ^{4}He," J. Low Temp. Phys. **208**, 475–481 (2022).
[12] T. Kamppinen, J. T. Mäkinen, and V. B. Eltsov, "Dimensional control of tunneling two-level systems in nanoelectromechanical resonators," Phys. Rev. B **105**, 035409 (2022).
[13] R. Blaauwgeers, M. Blazkova, M. Človečko, V. B. Eltsov, R. de Graaf, J. Hosio, M. Krusius, D. Schmoranzer, W. Schoepe, L. Skrbek, P. Skyba, R. E. Solntsev, and D. E. Zmeev, "Quartz tuning fork: thermometer, pressure-and viscometer for helium liquids," J. Low Temp. Phys. **146**, 537–562 (2007).
[14] M. Morishita, T. Kuroda, A. Sawada, and T. Satoh, "Mean free path effects in superfluid ^{4}He," J. Low Temp. Phys. **76**, 387–415 (1989).
[15] D. I. Bradley, P. Crookston, S. N. Fisher, A. Ganshin, A. M. Guénault, R. P. Haley, M. J. Jackson, G. R. Pickett, R. Schanen, and V. Tsepelin, "The damping of a quartz tuning fork in superfluid ^{3}He-B at low temperatures," J. Low Temp. Phys. **157**, 476–501 (2009).
[16] D. Schmoranzer, M. La Mantia, G. Sheshin, I. Gritsenko, A. Zadorozhko, M. Rotter, and L. Skrbek, "Acoustic emission by quartz tuning forks and other oscillating structures in cryogenic ^{4}He fluids," J. Low Temp. Phys. **163**, 317–344 (2011).
[17] J. Rysti and J. Tuoriniemi, "Quartz tuning forks and acoustic phenomena: Application to superfluid helium," J. Low Temp. Phys. **177**, 133–150 (2014).
[18] D. I. Bradley, M. Človečko, S. N. Fisher, D. Garg, E. Guise, R. P. Haley, O. Kolosov, G. R. Pickett, V. Tsepelin, D. Schmoranzer, and L. Skrbek, "Crossover from hydrodynamic to acoustic drag on quartz tuning forks in normal and superfluid ^{4}He," Phys. Rev. B **85**, 014501 (2012).
[19] A. M. Guénault, R. P. Haley, S. Kafanov, M. T. Noble, G. R. Pickett, M. Poole, R. Schanen, V. Tsepelin, J. Vonka, T. Wilcox, and D. E. Zmeev, "Acoustic damping of quartz tuning forks in normal and superfluid ^{3}He," Phys. Rev. B **100**, 104526 (2019).
[20] (Manufactured by the Statek Corporation, 512, N. Main Street, Orange, CA 92868, USA.).

[21]S. L. Ahlstrom, D. I. Bradley, M. Človečko, S. N. Fisher, A. M. Guénault, E. A. Guise, R. P. Haley, O. Kolosov, P. V. E. McClintock, G. R. Pickett, M. Poole, V. Tsepelin, and A. J. Woods, "Frequency-dependent drag from quantum turbulence produced by quartz tuning forks in superfluid ^{4}He," Phys. Rev. B **89**, 014515 (2014).

[22]D. Schmoranzer, M. J. Jackson, Š. Midlik, M. Skyba, J. Bahyl, T. Skokánková, V. Tsepelin, and L. Skrbek, "Dynamical similarity and instabilities in high-stokes-number oscillatory flows of superfluid helium," Phys. Rev. B **99**, 054511 (2019).

[23]D. I. Bradley, A. M. Guénault, V. Keith, C. J. Kennedy, I. E. Miller, S. G. Mussett, G. R. Pickett, and W. P. Pratt Jn., "New methods for nuclear cooling into the microkelvin regime," J. Low Temp. Phys. **57**, 359–390 (1984).

[24]D. J. Cousins, S. N. Fisher, A. M. Guénault, R. P. Haley, I. E. Miller, G. R. Pickett, G. N. Plenderleith, P. Skyba, P. Y. A. Thibault, and M. G. Ward, "An advanced dilution refrigerator designed for the new Lancaster microkelvin facility," J. Low Temp. Phys. **114**, 547–570 (1999).

[25]C. Bäuerle, Yu. M. Bunkov, S. N. Fisher, H. Godfrin, and G. R. Pickett, "Laboratory simulation of cosmic string formation in the early Universe using superfluid ^{3}He," Nature **382**, 332–334 (1996).

[26]K. Karrai and R. D. Grober, "Piezo-electric tuning fork tip—sample distance control for near field optical microscopes," Ultramicroscopy **61**, 197–205 (1995).

[27]S. Holt and P. Skyba, "Electrometric direct current I/V converter with wide bandwidth," Rev. Sci. Instrum **83**, 064703 (2012).

[28]E. Collin, T. Moutonet, J.-S. Heron, O. Bourgeois, Yu. M. Bunkov, and H. Godfrin, "A tunable hybrid electromagnetomotive NEMS device for low temperature physics," J. Low Temp. Phys. **162**, 653–660 (2011).

[29]S. N. Fisher, A. M. Guénault, C. J. Kennedy, and G. R. Pickett, "Beyond the two-fluid model: Transition from linear behavior to a velocity-independent force on a moving object in ^{3}He-B," Phys. Rev. Lett. **63**, 2566 (1989).

[30]D. I. Bradley, M. Človečko, S. N. Fisher, D. Garg, A. M. Guénault, E. Guise, R. P. Haley, G. R. Pickett, M. Poole, and V. Tsepelin, "Thermometry in normal liquid ^{3}He using a quartz tuning fork viscometer," J. Low Temp. Phys. **171**, 750–756 (2013).

[31]E. Varga, M. J. Jackson, D. Schmoranzer, and L. Skrbek, "The use of second sound in investigations of quantum turbulence in He-II," J. Low Temp. Phys. **197**, 130–148 (2019).

[32]W. R. Abel, A. C. Anderson, and J. C. Wheatley, "Propagation of zero sound in liquid He^3 at low temperatures," Phys. Rev. Lett. **17**, 74 (1966).

[33]D. Vollhardt and P. Wolfle, *The superfluid phases of helium 3* (Courier Corporation, 2013).

[34]J. Wilks, *The Properties of Liquid Helium* (Elsevier, 1966).

[35]H. L. Laquer, S. G. Sydoriak, and T. R. Roberts, "Sound velocity and adiabatic compressibility of liquid helium three," Phys. Rev. **113**, 417 (1959).